Available online at www.sciencedirect.com
SCIENCE DIRECT®
Analytica Chimica Acta 573–574 (2006) 9–13
ANALYTICA CHIMICA ACTA
www.elsevier.com/locate/aca

Metal oxide thin films as sensing layers for ozone detection

M. Suchea [a,c,*], N. Katsarakis [a,d], S. Christoulakis [a], M. Katharakis [d], T. Kitsopoulos [a,b], G. Kiriakidis [a,c]

[a] Institute of Electronic Structure and Laser, Foundation for Research and Technology-Hellas, P.O. Box 1527, 71110 Heraklion, Crete, Greece
[b] Department of Chemistry, University of Crete, Heraklion, Crete, Greece
[c] Department of Physics, University of Crete, Heraklion, Crete, Greece
[d] Center of Materials Technology and Laser, Science Department, School of Applied Technology, Technological Educational Institute of Crete, Heraklion, Estavromenos, 71004 Heraklion, Crete, Greece

Received 30 November 2005; received in revised form 10 April 2006; accepted 20 April 2006
Available online 29 April 2006

Abstract

In_2O_{3-x} thin films with a thickness of 100–990 nm were grown by dc magnetron sputtering. Their structural, electrical and ozone sensing properties were analyzed. Structural investigations carried out by electron probe micro analysis, secondary ion mass spectrometry and atomic force microscopy showed a strong correlation between stoichiometry, surface topology and gas sensitivity. Moreover, the electrical conductivity of In_2O_{3-x} thin films exhibited a change of over six orders of magnitude during photoreduction with ultraviolet light and subsequent oxidation in ozone atmosphere at room temperature.
© 2006 Elsevier B.V. All rights reserved.

Keywords: In_2O_{3-x} thin films; Stoichiometry; Ozone; Sensing

1. Introduction

Metal oxide semiconductors are suitable materials for gas sensors due to their low dimension, portability, and simplicity. The electrical properties of metal oxide thin films are strongly influenced by the presence of oxidizing and reducing gases. Oxidizing gases such as NO_2 and O_3 are common pollutant gases. It is well known that the gas adsorption onto the surface of a metal oxide semiconductor influences its electrical conductivity. In fact, conductivity of semiconductor gas sensors changes by a few orders of magnitude with respect to the initial value in the presence of gas concentrations up to few parts per million (ppm) in air at ambient pressure. It is also well known that electrical properties of semiconducting oxides like In_2O_{3-x} depend strongly on defect density created by external doping or distributed stoichiometry as well as their growth conditions [1–4]. A considerable amount of work has been reported on materials like In_2O_3 [4–9] to detect hydrocarbon gases, ozone, nitric oxide gases, ammonia, ethanol vapors etc but none of them have reported sensing of ozone below 50 ppb concentration. Using molecular field-effect transistors, however, ozone sensing below 10 ppb has been succeeded [10,11].

In this work, we report on the fabrication and surface, electrical and gas sensing characterization of In_2O_{3-x} thin films deposited by dc magnetron sputtering. We show that the films show gas sensing characteristics towards O_3 (50 ppb) at operating temperatures from room temperature (RT) to 100 °C. The changes in the electrical conductivity of the films during the photoreduction with UV and subsequent oxidation in ozone are correlated with the surface parameters of the films. We conclusively prove through electron probe micro analysis (EPMA) and secondary ion mass spectrometry (SIMS) measurements that film stoichiometry changes within the top 5 nm of the In_2O_{3-x} films. It can be thus concluded that the electrical conductivity changes and consequently the gas sensing properties of the films are a surface phenomenon.

2. Experimental

The depositions of the In_2O_{3-x} films were carried out in an Alcatel dc magnetron sputtering system using a 99.999% pure In

* Corresponding author. Tel.: +30 2810 391272; fax: +30 2810 391305.
E-mail address: mirasuchea@iesl.forth.gr (M. Suchea).

0003-2670/$ – see front matter © 2006 Elsevier B.V. All rights reserved.
doi:10.1016/j.aca.2006.04.057

metallic target under constant deposition parameters: the pressure was 8×10^{-3} mbar, the oxygen concentration in the plasma was 100%, the growth rate was 5.6 nm min^{-1} and the substrate temperature was kept at 27 °C. The base pressure in the chamber was 5×10^{-7} mbar. Films with thicknesses between 100 and 990 nm were deposited onto Corning 1737F glass substrates with electrical contacts and silicon substrates. The thickness was monitored in situ as well as ex situ using an Alphastep profilometer.

EPMA was carried out at University of Braunschweig, Germany using a CAMECA SX50 EPMA system under conditions ($E_0 = 5$ keV) where the depth of analysis was <150 nm. Available standards of InP (for In) and SnO_2 (for O) were used for quantification. SIMS was performed using a CAMECA IMS 5f system using the following experimental setup: 3 keV Cs^+ primary ions, Ip = 5 nA, raster 500 μm × 500 μm; Sputter rate 0.02 nm s^{-1} based on determination of crater depth by profilometry; CsM^+ (M = element of interest) molecular secondary ions, accepted area of Ø = 120 μm in the center of the raster field.

The surface morphology (grain size and surface roughness) was analyzed with a Nanoscope III atomic force microscope (Digital Co. Instruments, USA) using a normal silicon nitride tip (125 μm) in Tapping Mode scanning the surface with an oscillating tip to its resonant frequency (200–400 kHz). All measurements were made at RT. In the present study the RMS roughness of the surface is defined as: RMS (nm) = $[\sum(z_i - z_{ave})^2/N]^{1/2}$, where z_i is the current value of z, z_{ave} the mean value of z in the scan area, and N is the number of points. Grain radius and features dimensions were evaluated using the cross section analysis menu facilities of NanoScope III Program. The conductivity measurements were carried out in a special designed reactor [9] at RT in a home made system at FORTH. For photoreduction the samples were directly irradiated in vacuum by the UV light of a mercury pencil lamp at a distance of approximately 3 cm for 15 min in order to achieve a steady state. For the subsequent oxidation ozone was produced up-stream in the presence of UV and the chamber was backfilled with oxygen and ozone at a pressure of 560 Torr. This treatment lasted 45 min, after which no further changes of the conductivity could be observed. Finally, the chamber was evacuated and the photoreduction–oxidation cycle described above was repeated a few times. An electric field (1 or 10 V cm^{-1}) was applied during the whole cycling procedure to the samples and the electrical current was measured with an electrometer. Current–voltage (*I–V*) measurements were always performed before the cycling started in order to ensure the Ohmic nature of the contacts. The measurements in air/gas mixtures were performed using INDOORTRON facilities at the European Joint Research Centre at Ispra in Italy. The INDOORTRON is a walk-in type environmental chamber of a 30 m^3 volume featuring the ability to independently control temperature, relative humidity and air exchange rate. All the measurements were done under stationary conditions. Gas concentrations in the chamber were determined using gas spectroscopy. Photoreduction of the analyzed films was done using a solar lamp.

Table 1
Film stoichiometry was investigated by EPMA

Sample	In (at.%)	O (at.%)	In/O atomic ratio	Formula
In_2O_{3-x} non-conductive	40.5	59.5	0.68	$In_2O_{2.94}$
In_2O_{3-x} conductive	40.8	59.2	0.69	$In_2O_{2.90}$

3. Results and discussion

In_2O_{3-x} in its stoichiometric form (In_2O_3) behaves as an insulator, while in its non-stoichiometric form (In_2O_{3-x}), it appears to have semiconducting properties. Film stoichiometry was investigated by EPMA. The average of 15 points (spot ∼Ø = 10 μm) of analysis on each sample is presented in Table 1. In_2O_{3-x} non-conductive is considered to be the film as deposited, In_2O_{3-x} conductive is considered to be the film after UV exposure.

Within the precision of the EPMA experiments the "bulk" composition of the coatings has to be regarded as identical. The composition is very close to the stoichiometry of In_2O_3. For SIMS measurements the calibration of the concentration axis in respect of In and O was carried out by assuming the "bulk" stoichiometry (i.e., for a depth <20 nm) of $In_2O_{2.94}$ ($c_{In}/c_O = 0.68$) corresponding to the results of EPMA. The concentrations of impurity elements (H, C, N, Si) are rough estimations based on sensitivity factors derived from a coating standard of Si–C:H:N:O. Fig. 1a and b shows that both samples are homogeneous in depth. No difference between In_2O_{3-x} "non-conducting" and "conducting" is visible, including the level of impurity elements.

Fig. 2a and b give a "closer look" to the In and O concentrations in the near-surface region. Within a depth of 0–5 nm a small difference between In_2O_{3-x} "non-conducting" and "conducting" can be detected. This difference becomes clearly visible when the In:O atomic ratio of both samples is plotted as a function of depth (Fig. 3). As compared with the "bulk" (>10 nm) composition (In:O = 0.68 ⇒ $In_2O_{2.94}$), the sample "non-conducting" exhibits a surplus of O (2 nm: In:O ∼ 0.65, ∼$In_2O_{3.08}$) within the first 5 nm, whereas the sample "conducting" shows a deficit of O (2 nm: In:O ∼ 0.70, ∼$In_2O_{2.86}$).

The mechanism responsible for the conductivity changes in In_2O_{3-x} films is the formation and annihilation of oxygen vacancies. UV irradiation of the sample with energies above the bonding energy between In and O leads to a transformation of an oxygen atom from a bound state to the gaseous state [12]. This reflects in an increased electrical conductivity (σ_{max}) or a decreased resistivity (ρ). Subsequent exposure of the film to oxidizing gases will cause a surface interaction with the oxygen deficient metal oxide leading to a decrease of the electrical conductivity to a minimum value (σ_{min}), which can be correlated with the gas concentration. A typical photoreduction/oxidation cycle for In_2O_{3-x} films is shown in Fig. 4. All these interactions take place on the film near surface region (0–5 nm depth) as is shown from SIMS analysis in Fig. 3. In order to correlate the film surface properties with the film sensitivity to ozone (calculated as $\sigma_{max}/\sigma_{min}$ from conductometric tests in an evacuated

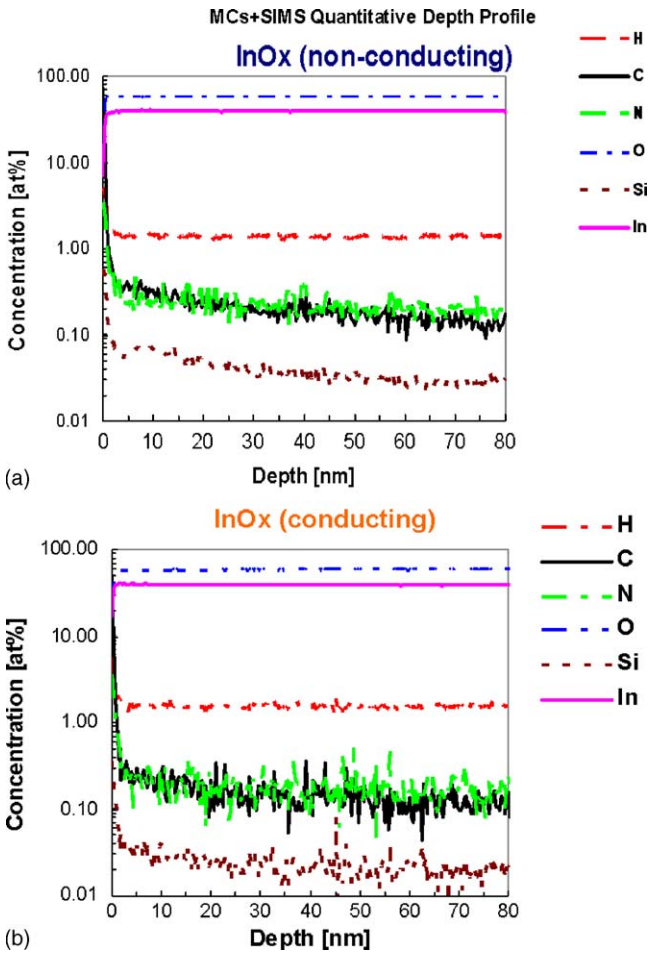

Fig. 1. SIMS compositional characterization of (a) "non-conducting" and (b) "conducting" In_2O_{3-x}. Calibration of the concentration axis in respect of In and O was carried out by assuming the "bulk" stoichiometry (i.e., for a depth < 20 nm) of $In_2O_{2.94}$ ($c_{In}/c_O = 0.68$) corresponding to the results of EPMA.

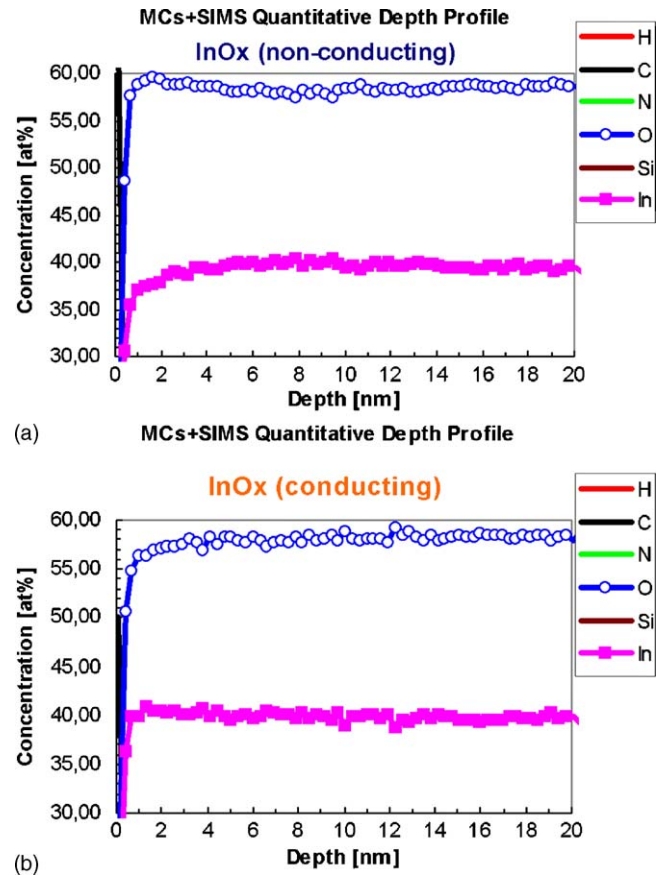

Fig. 2. A "closer look" to the In and O concentrations in the near-surface region. Within a depth of 0–5 nm a small difference between In_2O_{3-x} "non-conducting" (a) and "conducting" (b) can be detected.

chamber under a flow of O_3 at RT) we plotted the film sensitivity versus film thickness and the AFM measured surface parameters of grain radius (GR) and surface roughness (RMS) as it is shown in Fig. 5. These results are given for a film series with thickness varying from 100 to 990 nm. The correlation shows the strong influence of film thickness on topology and, consequently on film sensitivity. For increasing thicknesses from 100 to 648 nm and finally 990 nm, the $\sigma_{max}/\sigma_{min}$ ratio decreases from 10^6 to 2.1×10^4 and 3.3×10^3, respectively. This is a significant alteration of sensitivity. AFM images of film surfaces are shown in Fig. 6a–c. The RMS and GR are increasing with increasing film thickness. The film sensitivity correlation with the surface parameters can be explained using the conduction model of metal oxide gas sensors approximation given by Barsan and Weimar [13]. The mechanism of gas detection is the interaction of the gaseous species with the oxygen deficient surface of the semiconducting sensitive metal oxide layer. As a consequence of this surface interaction charge transfer takes place between the absorbed species and the semiconducting sensitive material. According to this model, for small grains and narrow necks, when the mean free path of free charge carriers become comparable with the dimension of the grains, the surface influence on the mobility becomes dominant over bulk phenomena. In the presence of the ionic species on the surface, after UV photoreduction, the electronic concentration in the surface states increases. The surface states concentration is correlated with the roughness and grain size via surface-to-volume ratio. Therefore, the gas sensitivity is strongly dependent on the film roughness and surface grain dimensions proving the importance of surface-to-volume ratio for high sensitivity applications. Increasing grain radius was found to reflect on decreasing sensitivity of our films mainly due to an increase of the film stoichiometry controlled by deposition parameters.

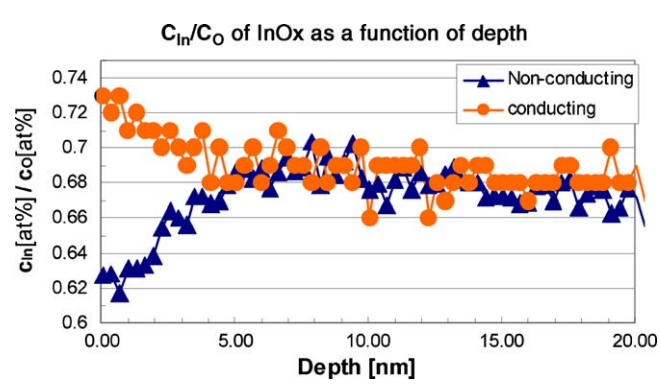

Fig. 3. In:O atomic ratio of both, "non-conducting" and "conducting" samples plotted as a function of depth.

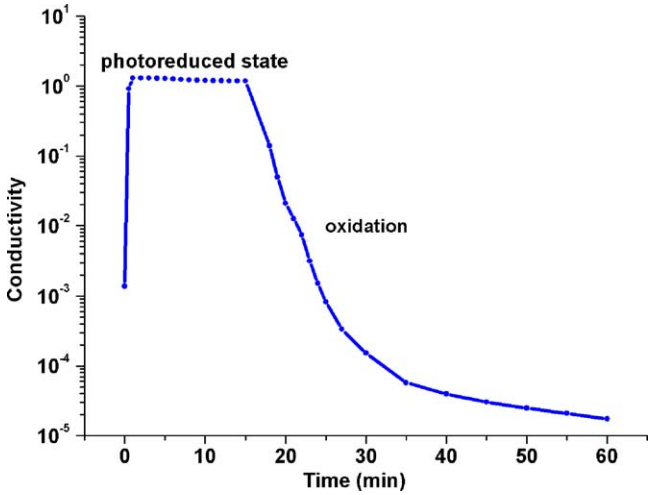

Fig. 4. A typical photoreduction/oxidation cycle for In_2O_{3-x} films.

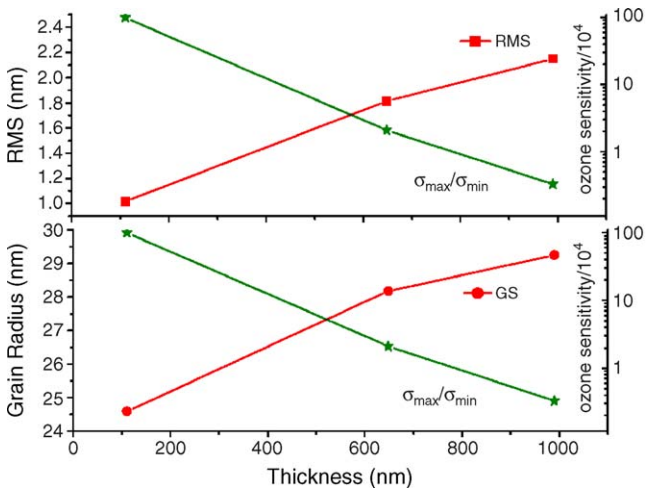

Fig. 5. The film sensitivity vs. film thickness and the AFM measured surface parameters surface roughness (RMS) and grain radius (GR).

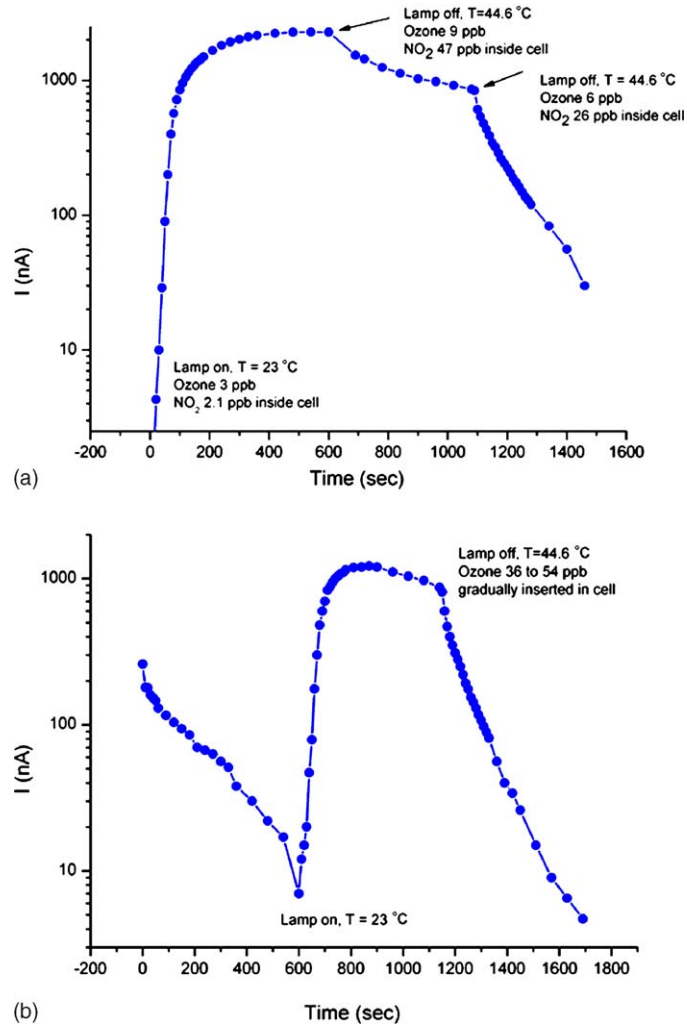

Fig. 7. Current measurements for the 110 nm In_2O_{3-x} film toward NO_2 (a) and O_3 (b) in air. The measurements were done without external heating under 1 V cm^{-1} electric field applied on the sample.

In Fig. 7a the electrical measurements for a 110 nm In_2O_{3-x} film in air/NO_2 mixture are presented. The measurements were done without external heating under 1 V cm^{-1} electric field applied on the sample. Photoreduction of the film was done using a solar lamp. The NO_2 concentration was varied from 2.1 to 47 parts per billion (ppb) in the presence of 3–9 ppb O_3 created from the interaction of UV light with air in the chamber. Photoreduction of the film causes a current increase of more than three orders of magnitude while consequent NO_2 oxidation leads to a decrease of the current by around two

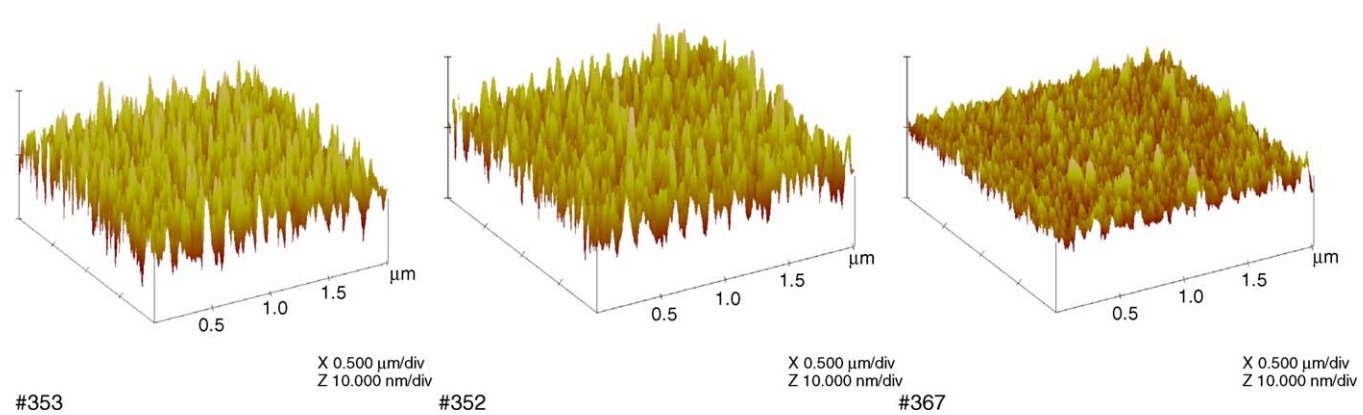

Fig. 6. AFM 3D images of different thickness film surfaces: (a) 990 nm, (b) 648 nm, (c) 110 nm. Scan size 2 µm × 2 µm, *X*-axis: 0.5 µm div^{-1}, *Z*-range: 10 nm div^{-1}.

orders of magnitude. Fig. 7b shows the electrical measurements for the same 110 nm In_2O_{3-x} film in an air/O_3 mixture. The ozone concentration was varied from 36 to 54 ppb in the presence of 5.4 ppb NO_2 and 0.2 ppb NO in air. It can be seen that photoreduction leads to a three orders of magnitude increase in the current, while subsequent oxidation in ozone causes an abrupt current decrease by more than three orders of magnitude. It can be noted that the changes in the film's conductivity are much larger when the photoreduction is done in vacuum and the oxidation in pure oxidizing gas atmosphere (see Fig. 4). During the whole process the temperature varied from 23 to 44.6 °C due to the heat released by the lamp. However, this small temperature variation in the chamber is the same for all measurements performed and does not influence significantly the film's response to the oxidizing gases.

The sensitivity of In_2O_{3-x} thin films grown by dc magnetron sputtering towards ozone in sub 50 ppb concentration in air is higher than for NO_2. The as-deposited In_2O_{3-x} thin films are not selective gas sensors; however, they show different response behavior for the oxidizing gases studied here, i.e., O_3 and NO_2. A possible way to make them selective might be to modify their surface [14].

4. Conclusions

Thin films of In_2O_{3-x} for ozone and nitrogen dioxide sensing applications have been successfully fabricated using dc magnetron sputtering. We have proved the stoichiometry role on film sensing properties as well as the fact that sensing is a surface phenomenon and it is strong connected with film surface parameters, which can be controlled by deposition parameters. The In_2O_{3-x} films show stable and repeatable gas sensing characteristics towards both O_3 and NO_2 at operatin temperatures from RT to 100 °C.

Acknowledgments

This work was supported by ASSEMIC MRTN-CT-2003-504826 and 3rd Gen LAC No NNE5-2001-00961 European funded projects and PENED 2003-03ED733 National funded project.

References

[1] J.J. Prince, S. Ramamurthy, B. Subramanian, C. Sanjeeviraja, M. Jayachandran, J. Cryst. Growth 240 (2002) 142.
[2] S. Muranaka, Y. Bando, T. Takada, Thin Solid Films 151 (1987) 353.
[3] V.D. Das, S. Kirupavathy, L. Damodare, N. Lakshminarayan, J. Appl. Phys. 79 (1996) 8521.
[4] M. Girtan, G. Rusu, Analele Stintifice Ale Universitatii, Al. I. Cuza Din Iasi Tomul XLV-XLVIs Fizica Starii Condenstate, 1999–2000, p. 166.
[5] T. Takada, K. Suzuki, M. Nakane, Sens. Actuators B 13 (1–3) (1993) 404.
[6] C.N.R. Rao, A.R. Raju, K. Vijaymohan, New Materials, Narosa Publishing House, New Delhi, 1992, p. 1 (chapter 1).
[7] H. Fritzche, B. Pashmakov, B. Claflin, Solar Energy Mater. Solar Cells 32 (1994) 383.
[8] K.K. Makhija, A. Ray, R.M. Patel, U.B. Trivedi, K.N. Kapse, Bull. Mater. Sci. 28 (2005) 9.
[9] M. Bender, N. Katsarakis, E. Gagaoudakis, E. Hourdakis, E. Douloufakis, V. Cimalla, G. Kiriakidis, J. Appl. Phys. 90 (2001) 5382.
[10] M. Bouvet, Anal. Bioanal. Chem. 384 (2006) 366.
[11] M. Bouvet, G. Guillaud, A. Leroy, A. Maillard, S. Spirkovitch, F. Tournilhac, Sens. Actuators B 73 (2001) 63.
[12] S. Mishra, C. Ghanshyama, N. Rama, R.P. Bajpai, R.K. Bedi, Sens. Actuators B 97 (2004) 387.
[13] N. Barsan, U. Weimar, J. Electroceram. 7 (2001) 143.
[14] G. Korotcenkov, V. Golovanov, V. Brinzari, A. Cornet, J. Morante, M. Ivanov, J. Phys.: Conf. Ser. 15 (2005) 256.